Journal of Magnetism and Magnetic Materials 394 (2015) 463–469

Contents lists available at ScienceDirect

Journal of Magnetism and Magnetic Materials

journal homepage: www.elsevier.com/locate/jmmm

Electronic structure and magnetism of new ilmenite compounds for spintronic devices: $FeBO_3$ (B = Ti, Hf, Zr, Si, Ge, Sn)

R.A.P. Ribeiro [a], A. Camilo Jr.[b], S.R. de Lazaro [a,*]

[a] Department of Chemistry, State University of Ponta Grossa, Av. General Carlos Cavalcanti, 4748, 84030-900 Ponta Grossa, PR, Brazil
[b] Department of Physics, State University of Ponta Grossa, Av. General Carlos Cavalcanti, 4748, 84030-900 Ponta Grossa, PR, Brazil

ARTICLE INFO

Article history:
Received 7 November 2014
Received in revised form
13 May 2015
Accepted 27 May 2015
Available online 6 July 2015

Keywords:
DFT
Ilmenite
Spintronic
Half-metallicity
Semiconductor

ABSTRACT

First-principles calculations were performed in the framework of Density Functional Theory (DFT) within hybrid functional (B3LYP) to study the electronic structure and magnetic properties of new ilmenite $FeBO_3$ (B=Ti, Hf, Zr, Si, Ge, Sn) materials. In particular, the magnetic exchange interaction between Fe^{2+} layers is dependent on the interlayer distance and it can be controlled by ionic radius of B-site cation. Thus, Fe(Ti, Si, Ge)O_3 are antiferromagnetic materials, while Fe(Zr, Hf, Sn)O_3 are ferromagnetic. We also argue that antiferromagnetic materials and $FeZrO_3$ are convectional semiconductors, whereas $FeHfO_3$ and $FeSnO_3$ exhibit intrinsic half-metallic behavior, making them promising candidates for spintronic devices.

1. Introduction

In recent years, the scientific interest on the development of devices in the field of spintronic has been intensified. The performance of these devices depends on the spin polarization of the current used for information storage [1]. The most promising candidates for these applications have a semiconductor behavior with respect to the electrons with a spin orientation, whereas they are metallic in relation to inverse spin orientation, being denominated Half-Metallic Ferromagnets (HFMs) [2,3]. Recently, a lot of theoretical and experimental studies have been developed to investigate various HFMs materials, such as metallic oxides (CrO_2, Fe_3O_4) [4,5] perovskites manganites and double-perovskites (Bi_2FeMoO_6, Bi_2MnMoO_6, etc.) [6], zinc-blend compounds (CrAs, CrSb, TiSb, CaC, etc.) [7–9] and Heusler alloys [10–13].

In many of these materials, the spin injection is the result of a complex mixture of transition metals that do not present usual crystalline structures for semiconductor industry, for instance, double-perovskites and metastable zinc-blende materials [14,15]. In other cases, extensive doping with rare-earth elements and transition metals is required hindering the application due to the increase in costs in production process and the presence of huge holes' concentration that does not prevent controlled doping independent of magnetism [16]. Nowadays, Heusler alloys are the most researched materials in the field of spintronic [10]. However, because of the tendency towards device miniaturization and the large variety of physical properties, transition-metal oxides as ABO_3 compounds provide large advantages for spintronics [15]. Recently, despite the fact that main candidates investigated for spintronic applications are ferromagnetics, other magnetic materials (antiferromagnetic) have been the subject of scientific interest. In comparison to the ferromagnetics, such materials have several advantages such as the capability to operate at higher frequencies (terahertz) enabling the creation of high-speed devices. Furthermore, antiferromagnetic materials are commonly semiconductors making it possible to combine the electronic and spintronic multi-functionality in a single device [17–19].

From this point of view, in the present work we propose new half-metallic materials design based on antiferromagnetic semiconductor $FeTiO_3$. Such ilmenite structure is derived from Corundum (R_2O_3) structure having an oxygen close-packing array, in which the cations occupy two thirds of the octahedral interstices with R-3 (n 148) space group. Octahedral sites are ordered in two non-equivalent layers consisting of alternated planes from Fe^{2+} and Ti^{4+} cations in the [001] direction and are connected to oxygen atoms [20–22]. This intermetallic connection is essential to the development of ferroelectric and magnetic properties on crystalline structure providing potential applications in electronic and opto-electronic devices, high temperature integrated circuits,

* Corresponding author.
E-mail address: srlazaro@uepg.br (S.R. de Lazaro).

http://dx.doi.org/10.1016/j.jmmm.2015.05.096
0304-8853/

Table 1
Theoretical and experimental results for lattice parameters (in Å), unit cell volume (V, in Å^3), total energy difference between different magnetic ordering (E, in meV) and total magnetic moments (μT, in μB) of $FeBO_3$ (B=Ti, Hf, Zr, Si, Ge, Sn) materials.

Models	Lattice parameters			ΔE_{AFM-FM}	μ_T
	a	*c*	*V*		
$FeTiO_3$	5.093	14.226	319.61	−45.8	0.0
$FeZrO_3$	5.453	14.242	366.69	63.3	7.61
$FeHfO_3$	5.414	14.158	359.40	54.2	7.65
$FeSiO_3$	4.762	14.191	278.67	−32.1	0.0
$FeGeO_3$	5.013	14.227	309.61	−17.0	0.0
$FeSnO_3$	5.275	14.437	347.92	94.8	7.65
Theoretical ($FeTiO_3$)[a]	5.150	14.095	320.27	–	–
Experimental ($FeTiO_3$)[b]	5.087	14.083	316.08	–	–

[a] Ref. [45].
[b] Ref. [43].

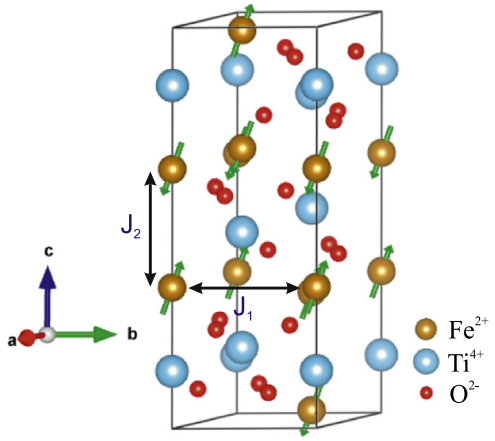

Fig. 1. The crystalline structure for $FeTiO_3$. J_1 and J_2 refer to the magnetic interactions in the intralayers and interlayers, respectively. Arrows illustrate the orientation of magnetic moments (μ) on antiferromagnetic alignment.

photocatalysis and others [20,23–27]. Several other mixed oxides adopt the ilmenite structure, for example, $ZnSnO_3$, $CdSnO_3$, $FeGeO_3$, $MgSiO_3$, etc. [28–31]. However, there are no theoretical or experimental reports about electronic and magnetic properties from Fe-based on ilmenite materials, such as $FeSiO_3$, $FeSnO_3$, $FeGeO_3$, $FeHfO_3$ and $FeZrO_3$.

2. Computational methodology

Extensive experimental routines are required to investigate the half-metallic behavior in HFMs materials, [32–35] therefore, it is not surprising that electronic-structure quantum calculations continue to play an important role in research of new HFMs design [3]. Then, we carried out first-principles calculations based on Density Functional Theory (DFT) using hybrid functional of a non-local exchange functional developed from Becke [36,37] combined with a correlation functional based on gradient of electronic density developed from Lee, Yang and Parr (B3LYP) [38] and implemented in CRYSTAL09 package [39]. The basis set used for describing Fe, Ti, Zr, Si, Ge and O atoms were composed by Gaussian type functions with Triple-Zeta polarization (TZVP) studied by Peintinger and co-workers [40] and for Sn, Hf atom it was used pseudopotential basis set Sn-DURAND-21G* and Hf-ECP-411d31G, respectively [41,42]. The crystalline structures for $FeBO_3$ (B=Ti, Hf, Zr, Si, Ge, Sn) materials were based on experimental parameters of $FeTiO_3$ material [43]. Both ferromagnetic (FM) and antiferromagnetic (AFM) orderings were calculated for these materials. All optimizations were performed in relation to the system total energy using mono and bielectronic intregals converged with pre-defined criteria in 10^{-8} Hartree. The diagonalization of the matrix density was carried out using the grid of k points in reciprocal space according to the Monkhorst–Pack method [44] and the shrink factor was set to 6 × 6 (Gilat Web) corresponding to 40 independent points k in the Brillouin zone.

3. Results and discussion

3.1. Structural properties

In order to determine the equilibrium lattice parameters of $FeBO_3$ (B=Ti, Hf, Zr, Si, Ge, Sn) materials, the total energy was optimized as a function of unit cell volume for ferromagnetic (FM) and antiferromagnetic (AFM) orderings. The theoretical results obtained from this procedure are shown in Table 1. Regarding magnetic ordering in ilmenite structure, the positive value of ΔE indicates that the FM state is more favorable, whereas negative value indicates that the AFM state is more stable. Theoretical results (Table 1) show that for $FeTiO_3$, $FeSiO_3$ and $FeGeO_3$ the AFM state is more favorable, insofar the FM state is more favorable for $FeZrO_3$, $FeHfO_3$ and $FeSnO_3$ materials.

$FeTiO_3$ is widely known to be an antiferromagnetic material. In ilmenite structure the Fe and Ti chains are distributed in alternating planes. For magnetic cations (Fe^{2+}) the structural arrangement provides different exchange interactions, as shown in Fig. 1. For intrasublattice the Fe^{2+} interactions, experimental evidences suggest a parallel ordering (FM) of spins (J_1=28.5 K), whereas for intersublattice Fe^{2+} it is observed an antiparallel (AFM) alignment of magnetic moments (J_2=−6.67 K). This AFM ordering mainly occurs due to the interlayers Fe–Fe direct exchange vanishing the total magnetic moment for $FeTiO_3$ (μ_T=0). Unlike interlayer interactions, intrasublattice magnetic exchange is indirect, where Fe^{2+} atoms are mediated by the diamagnetic oxygen through the overlap of the metal 3d and oxygen 2p orbitals. Thus, it is possible to assume that oxygen 2p orbitals act as a barrier between the neighboring Fe^{2+} atoms providing a parallel alignment.

From an inspection of results shown in Table 1 it is possible to note that increasing the ionic radius of B-cations in the ilmenite structure, the energy difference between AFM and FM states increases linearly because the larger distance between Fe^{2+} layers favors the parallel coupling in the [0001]-axis. This linear behavior as a function of distance is characteristic of direct exchange between neighboring magnetic cations [46]. However, the main influence of the ionic radius of B-site cation is observed in the overlap between the d orbitals of neighboring layers of Fe^{2+}, which is reduced giving rise to the ferromagnetism. Lattice parameters obtained for $FeTiO_3$ material are in accordance to the experimental results and the deviations are similar to other theoretical studies [45]. From these theoretical results it can be seen that unit cell volume is modified according to ionic radius of atoms localized in the B site due to bond distance difference. Nevertheless, the symmetry of the ilmenite was kept fixed for all models. The calculated magnetic moments for ferromagnetic $FeBO_3$ materials suggest a magnetic localization, which is not changed in relation to cation modification in the B-site. Our calculations show that the magnetic moments on Fe^{2+} are 3.81 μB, 3.83 μB and 3.83 μB for $FeZrO_3$, $FeHfO_3$ and $FeSnO_3$, respectively; and are in accordance to $3d^6$ electronic configuration of the Fe^{2+} cation.

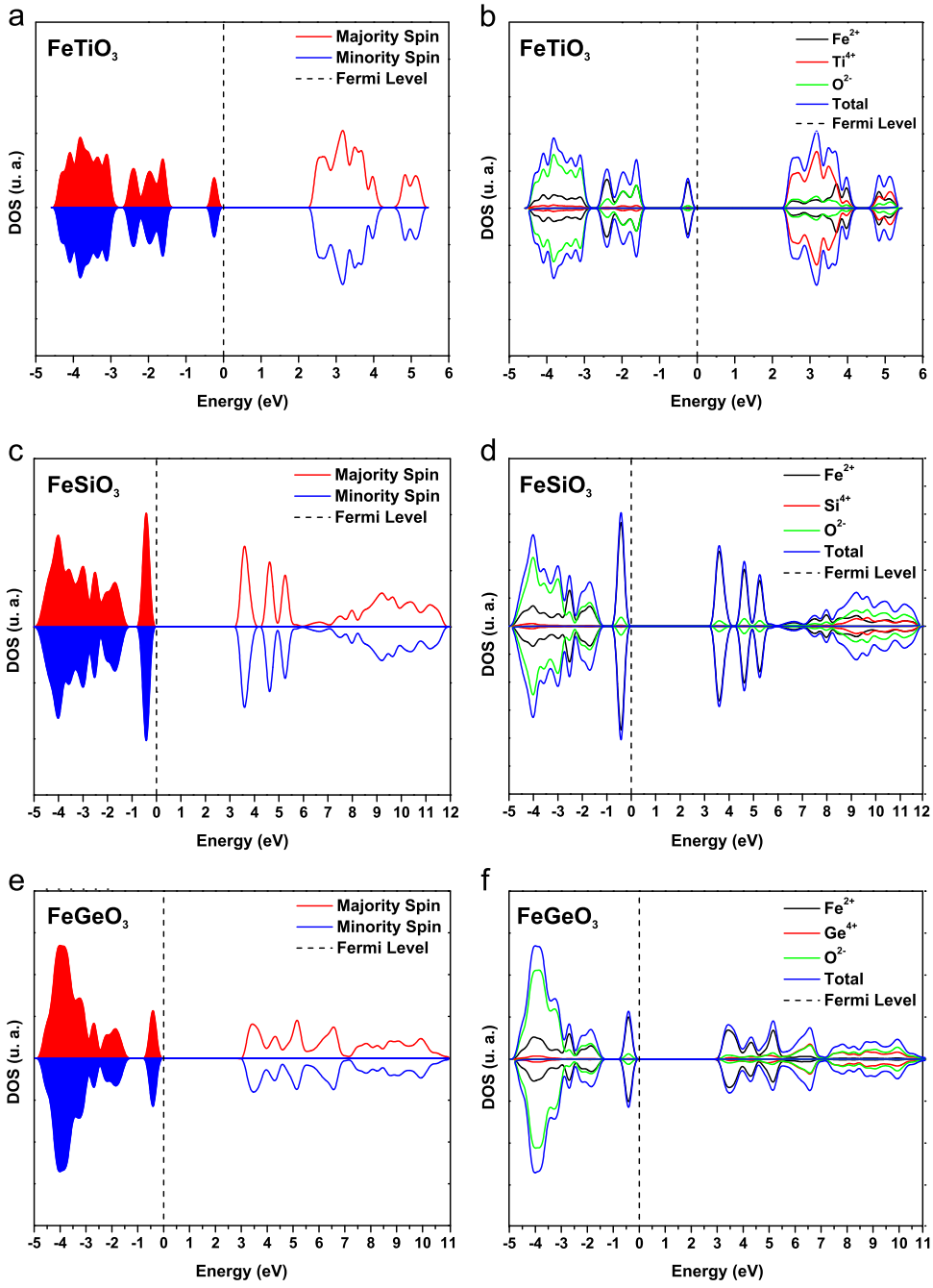

Fig. 2. Spin-polarized atom-resolved density of states for $FeTiO_3$, $FeSiO_3$ and $FeGeO_3$ antiferromagnetic materials . The Fermi levels were all set to zero.

3.2. *Electronic properties*

To investigate the electronic properties of $FeBO_3$ (B=Ti, Hf, Zr, Si, Ge, Sn) materials, the spin-polarized total and atom-resolved Density of States (DOS) (Fig. 2) and Band Structure profiles (Fig. 3) were calculated at their equilibrium lattice parameters. For this study, the materials were divided according to their magnetic behavior in the ground state.

3.2.1. *Antiferromagnetic materials*

Antiferromagnetic materials represent the majority of magnetically ordered compounds present in nature. However, the use of these materials for the technological industry is reduced to improve the hardness of ferromagnetic electrodes through the exchange-bias effect [47]. At the same time, it is believed that such materials may be useful in the replacement of ferromagnetic compounds in production of ultra-fast and ultrahigh-density spintronics devices due to rigidity to external magnetic fields and the absence of stray fields [18,19]. Energetic calculations demonstrate that $FeTiO_3$, $FeSiO_3$ and $FeGeO_3$ have antiferromagnetic ground state (Table 1).

From total DOS results for antiferromagnetic materials (Fig. 2) it is noted that for both, majority (↑) and minority (↓) spin states, the valence band (VB) is composed predominantly of O (2p) and Fe (3d, 4s, 4p) atomic states, whereas the Fe (3d, 4s, 4p) and Ti (3d, 4s, 4p) and Si (3s, 3p, 3d) and Ge (4s, 4p, 4d) atomic states contribute predominantly for the conduction band (CB). Regarding to energy range of maximum and minimum of valence (VBM) and conduction

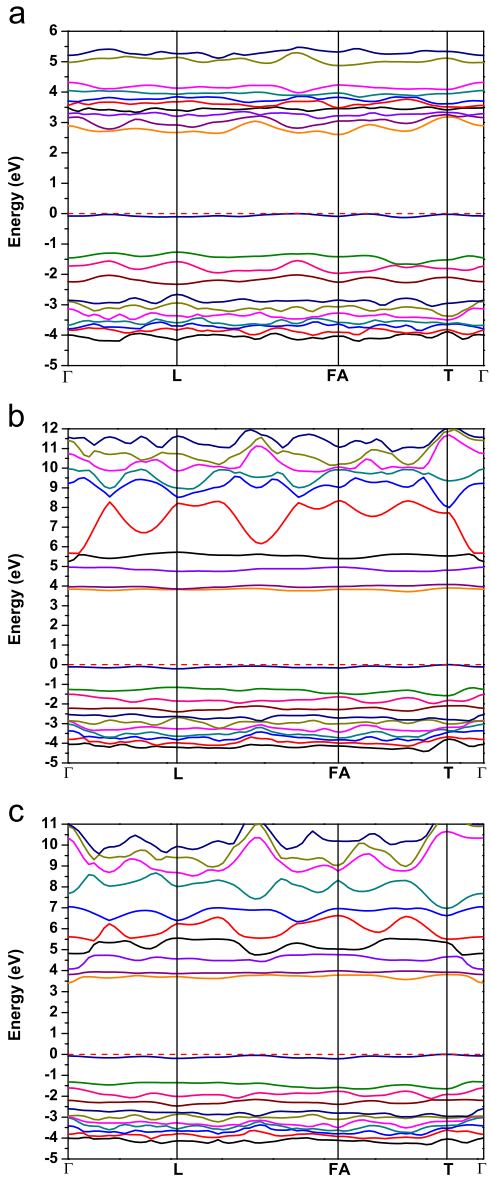

Fig. 3. Band structure for antiferromagnetic materials. (a) $FeTiO_3$, (b) $FeSiO_3$ and (c) $FeGeO_3$ materials. The Fermi levels were all set to zero.

band (CBM), respectively; it was observed that for $FeSiO_3$ and $FeGeO_3$ materials the CBM is shifted to higher energy, in comparison to $FeTiO_3$. This result can be attributed to the greater electronegativity of Si and Ge cations, which increases the covalent character of Si–O and Ge–O bonds in comparison to Ti–O. Similar results are found for other kind of materials [48–50].

As discussed above $FeBO_3$ (B=Ti, Si, Ge) are antiferromagnetic materials, so the band structure of the two spin-channels are similar and, consequently, one spin-channel has been reported, as shown in Fig. 3.

We found that $FeTiO_3$, $FeSiO_3$ and $FeGeO_3$ show a semiconducting behavior with an indirect band-gap of 2.60 (T-FA), 3.84 (T-Γ) and 3.41 (T-Γ) eV, respectively. The calculated band-gap for $FeTiO_3$ is in accordance to the experimental results (2.5–2.8 eV) [27]. Furthermore, it was observed that replacing Ti^{4+} by Si^{4+} and Ge^{4+} cations, the CBM is shifted to a higher energy increase in the band-gap. This cation modification changes the band energies in the different points of Brillouin zone for the first electronic states of CBM, making them flat-bands and reducing the difference between direct and indirect band-gap (Fig. 5)

3.2.2. Ferromagnetic materials

Magnetic materials with parallel ordering of spins (ferromagnetics) are prime candidates for the solidification of spintronics. Nowadays, the principal aim of spintronics is to develop new multifunctional materials which exhibit a semiconductor and metallic behavior. A major difficulty is to discover materials that exhibit these properties intrinsically [1,51,52].

As well as for antiferromagnetic materials, the DOS for $FeZrO_3$, $FeHfO_3$ and $FeSnO_3$ exhibit the same pattern of distribution for electronic states in the valence band (VB) and conduction band (CB) with O (2p) and Fe (3d, 4s, 4p) predominantly in VB; whereas, the CB is mainly composed by B-site and Fe atomic states (Fig. 4). Furthermore, it indicates clearly that $FeZrO_3$ exhibit semiconductor behavior and $FeBO_3$ (B=Hf, Sn) materials show half-metallic behavior, being semiconductors with majority spin channels and metals in relation to opposite spin orientation. These results indicate typical half-metallic magnetism with 100% spin polarization at Fermi Level (EF).

From numerical integration methods, it is possible to calculate the number of electrons and holes in the VB and CB, respectively [53]. These results are shown in Table 2. For $FeZrO_3$ material the VB is occupied by $n=1.6\text{x}10^{24}$ e·cm^{-3} distributed on spin-up (81%) and spin-down channels (19%); whereas, the CB has $p=1.2$ x 10^{24} e·cm^{-3}, which are distributed on spin-up channels (25%) and spin-down channels (75%). The same behavior was observed to $FeHfO_3$ and $FeSnO_3$ models, indicating p-type semiconductor characteristics.

From band structure profiles (Fig. 5), it was observed that for all models, the spin-up channel has a semiconductor band-gap around 3.13, 5.89 and 3.79 eV for $FeZrO_3$, $FeHfO_3$ and $FeSnO_3$, respectively. Furthermore, the nature of the excitation in the $FeZrO_3$ and $FeHfO_3$ materials is an indirect band-gap at L-FA points (Fig. 5a–d); whereas, $FeSnO_3$ has a direct band-gap at Γ–Γ points (Fig. 5e and f). For spin-down channel it was observed that only $FeZrO_3$ has a semiconductor direct band-gap of 5.01 eV at FA–FA points, while $FeHfO_3$ and $FeSnO_3$ are metallic materials with band-gap around 0.10 and 0.37 eV, respectively. However, comparing band structure profiles for $FeZrO_3$ and $FeHfO_3$ materials, we can observe that the disturbance on VBM caused by the modification of the B-site cation is very subtle, making the semi-metallic behavior for $FeHfO_3$ dependent on thermal and magnetic oscillations. Such behavior can be proved by the half-metallic band-gap for these materials; $FeSnO_3$ has a larger band-gap (0.37 eV) in comparison to $FeHfO_3$ (0.10 eV) causing a falls for Fermi level in the band-gap only for iron stannate; while for $FeHfO_3$, the Fermi level moves to the top of the minority occupied states. Thus, theoretical band structure and DOS results suggest that ilmenite $FeSnO_3$ is a good candidate for spintronic applications due to the intrinsic half-metallic behavior.

4. Conclusions

We apply quantum calculations based on Density Functional Theory with B3LYP hybrid functional to predict the structural, electronic and magnetic properties of the $FeBO_3$ (B=Ti, Hf, Zr, Si, Ge, Sn) materials in ilmenite structure. Calculated lattice parameters for $FeTiO_3$ material are in accordance to experimental and theoretical results. Total energy calculation indicates that magnetic ordering for ilmenite structure is dependent to the distance of the Fe^{2+} layers in the (0001) direction canning be controlled by the ionic radius of B-site cation. The spin-polarized DOS results show

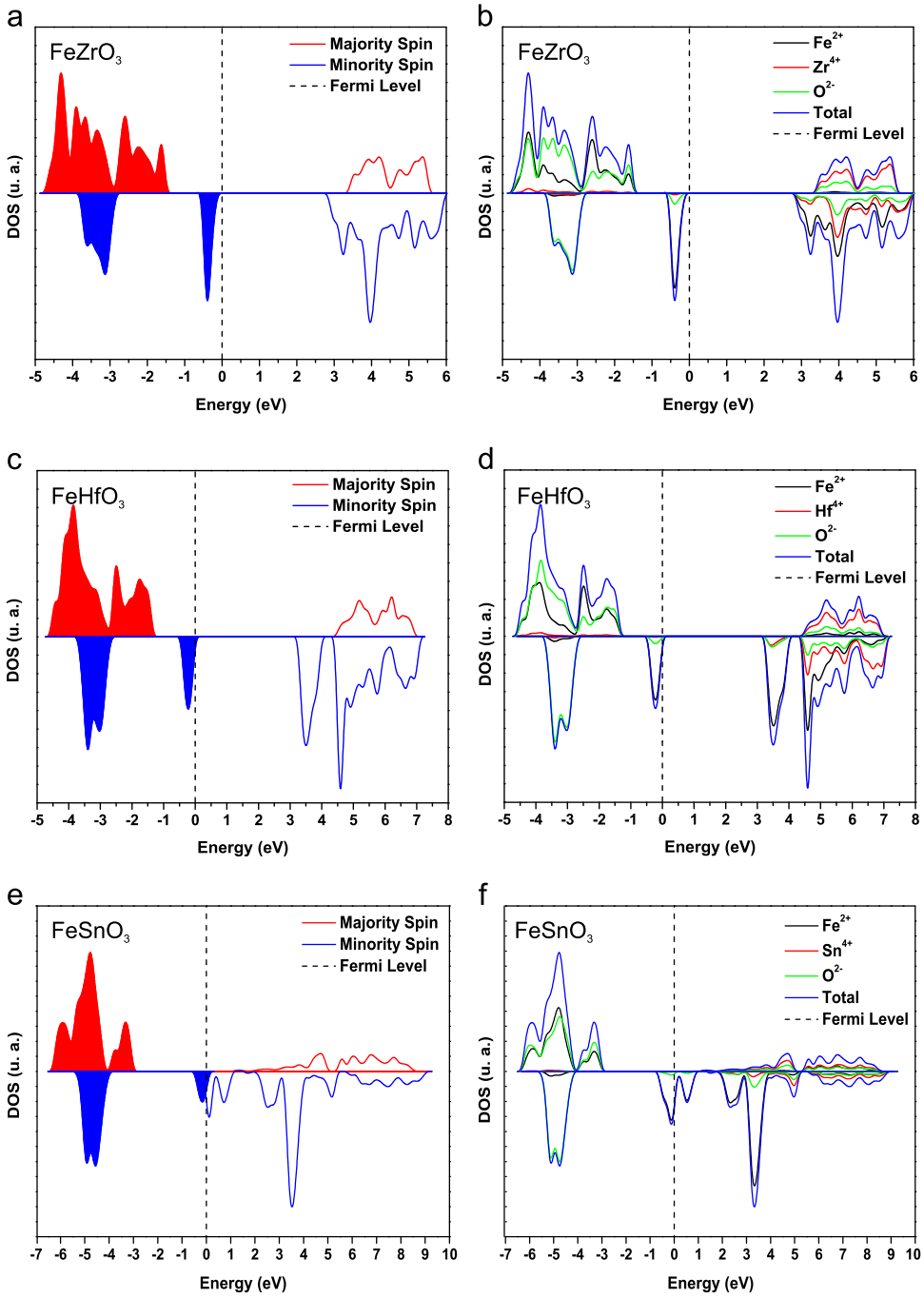

Fig. 4. Spin-polarized atom-resolved density of states for $FeZrO_3$, $FeHfO_3$ and $FeSnO_3$ ferromagnetic materials . The Fermi levels were all set to zero.

Table 2
Electrons (n) and hole (p) concentration ($n \cdot cm^{-3}$ and $p \cdot cm^{-3}$) for majority (↑) and minority (↓) spin of $FeBO_3$ (B=Zr, Hf, Sn) materials.

Models	n		p	
	Up	Down	Up	Down
$FeZrO_3$	1.3×10^{24}	3.2×10^{23}	2.8×10^{23}	9.0×10^{23}
$FeHfO_3$	1.1×10^{24}	4.4×10^{23}	3.5×10^{22}	9.0×10^{23}
$FeSnO_3$	9.6×10^{23}	6.9×10^{23}	1.1×10^{24}	3.9×10^{23}

that $FeTiO_3$, $FeZrO_3$, $FeSiO_3$ and $FeGeO_3$ materials exhibit a p-type semiconductor behavior, while $FeHfO_3$ and $FeSnO_3$ materials have showed half-metallic behavior for spin-down channels and p-type semiconductor characteristics for spin-up. Band structure calculations showed for half-metallic behavior of $FeHfO_3$ can be very sensitive to thermal and magnetic changes. Magnetic moment

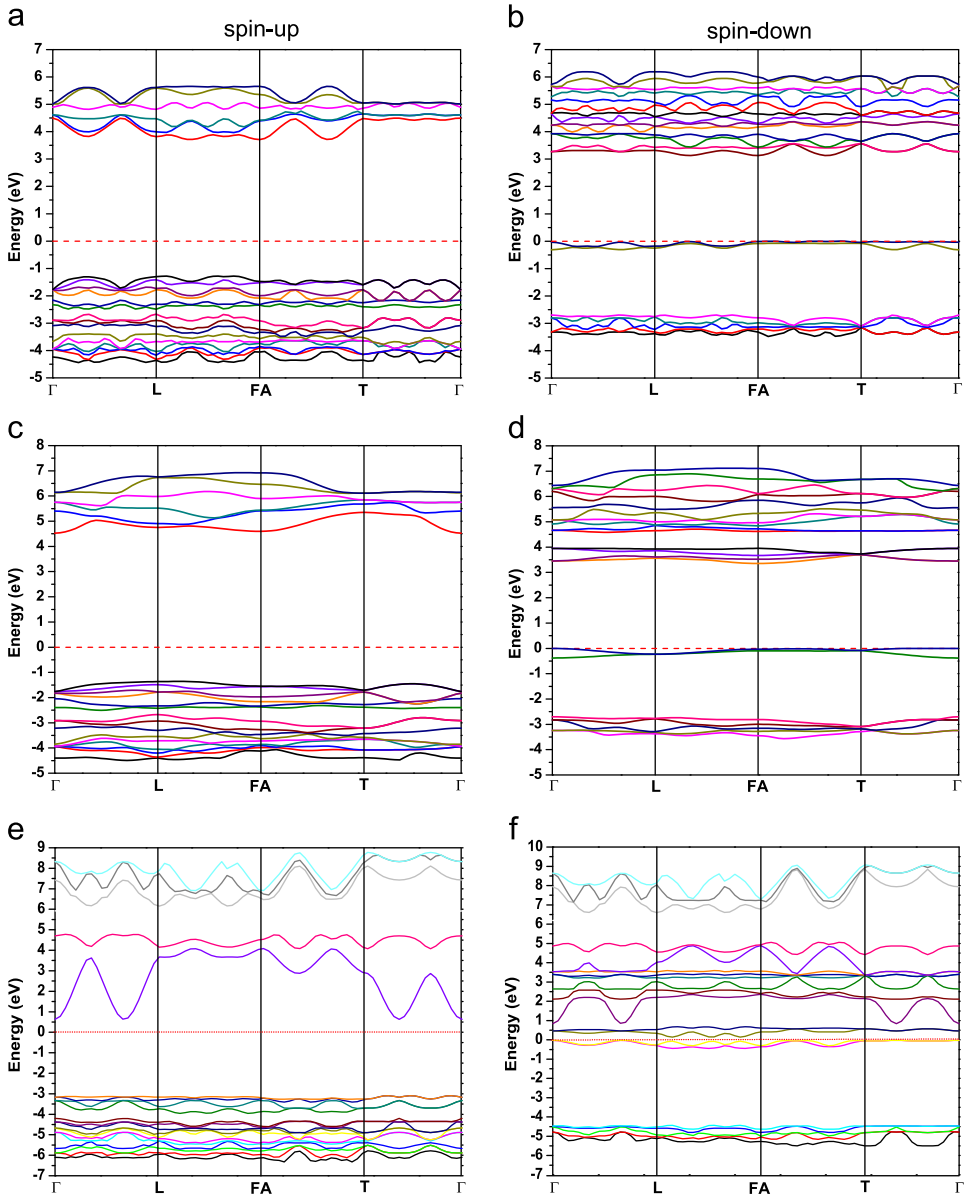

Fig. 5. Band structure of $FeZrO_3$ (a and b), $FeHfO_3$ (c and d) and $FeSnO_3$ (e and f) materials. Majority spin channel (spin-up) in the left hand side of the figure and minority spin channel (spin-down) in the right hand side. The Fermi levels were all set to zero.

results indicate that magnetic behavior is not modified through B-site modification, making $FeHfO_3$ and $FeSiO_3$ intrinsic half-metallic materials for potential applications in spintronic devices.

Acknowledgments

This research was financially supported by UEPG, CAPES and Fundação Araucária.

References

[1] K. Inomata, N. Ikeda, N. Tezuka, R. Goto, S. Sugimoto, M. Wojcik, E. Jedryka, Highly spin-polarized materials and devices for spintronics, Sci. Technol. Adv. Mater. 9(1) (2008) 014101. http://dx.doi.org/10.1088/1468-6996/9/1/014101. URL ⟨http://stacks.iop.org/1468-6996/9/i=1/a=014101⟩.

[2] C. Felser, G. Fecher, B. Balke, Spintronics: a challenge for materials science and solid-state chemistry, Angew. Chem. Int. Ed. 46(5) (2007) 668–699. http://dx.doi.org/10.1002/anie.200601815. URL ⟨http://dx.doi.org/10.1002/anie.200601815⟩.

[3] M.I. Katsnelson, V.Y. Irkhin, L. Chioncel, A.I. Lichtenstein, R.A. de Groot, Half-metallic ferromagnets: from band structure to many-body effects, Rev. Mod. Phys. 80(2) (2008) 315–378. http://dx.doi.org/10.1103/RevModPhys.80.315. URL ⟨http://link.aps.org/doi/10.1103/RevModPhys.80.315⟩.

[4] S.P. Lewis, P.B. Allen, T. Sasaki, Band structure and transport properties of CrO_2, Phys. Rev. B: Condens. Matter Mater. Phys. 55(16) (1997) 10253–10260. http://dx.doi.org/10.1103/PhysRevB.55.10253. URL ⟨http://link.aps.org/doi/10.1103/PhysRevB.55.10253⟩.

[5] R. Arras, L. Calmels, B. Warot-Fonrose, Half-metallicity, magnetic moments, and gap states in oxygen-deficient magnetite for spintronic applications, Appl. Phys. Lett. 100(3) (2012) 032403. http://dx.doi.org/10.1063/1.3678028. URL ⟨http://scitation.aip.org/content/aip/journal/apl/100/3/10.1063/1.3678028⟩.

[6] S.-D. Li, P. Chen, B.-G. Liu, Promising ferrimagnetic double perovskite oxides towards high spin polarization at high temperature, AIP Adv. 3(1) (2013) 012107. http://dx.doi.org/10.1063/1.4775352. URL ⟨http://scitation.aip.org/content/aip/journal/adva/3/1/10.1063/1.4775352⟩.

[7] C.Y. Fong, M.C. Qian, New spintronic superlattices composed of half-metallic compounds with zinc-blende structure, J. Phys.: Condens. Matter 16(48) (2004) S5669. URL ⟨http://stacks.iop.org/0953-8984/16/i=48/a=025⟩.

[8] G.Y. Gao, K.L. Yao, Bulk and surface half-metallicity: metastable zinc-blende TiSb, J. Appl. Phys. (Melville, NY, U. S.) 112(2) (2012) 023712. http://dx.doi.org/doi:http://dx.doi.org/10.1063/1.4739744. URL ⟨http://scitation.aip.org/content/aip/journal/jap/112/2/10.1063/1.4739744⟩.

[9] W.-H. Xie, B.-G. Liu, D.G. Pettifor, Half-metallic ferromagnetism in transition metal pnictides and chalcogenides with wurtzite structure, Phys. Rev. B: Condens. Matter Mater. Phys. 68(13) (2003) 134407. URL ⟨http://link.aps.org/doi/10.1103/PhysRevB.68.134407⟩.

[10] R. Umamaheswari, M. Yogeswari, G. Kalpana, Ab-initio investigation of half-metallic ferromagnetism in half-heusler compounds XYZ (X=Li, Na, K and Rb; Y=Mg, Ca, Sr and Ba; Z=B, Al and Ga), J. Magn. Magn. Mater. 350(0) (2014) 167–173. http://dx.doi.org/http://dx.doi.org/10.1016/j.jmmm.2013.09.019. URL ⟨http://www.sciencedirect.com/science/article/pii/S0304885313006690⟩.

[11] L. Xiong, L. Yi, G.Y. Gao, Search for half-metallic magnets with large half-metallic gaps in the quaternary Heusler alloys CoFeTiZ and CoFeVZ (Z=Al, Ga, Si, Ge, As, Sb), J. Magn. Magn. Mater. 360(0) (2014) 98–103. http://dx.doi.org/http://dx.doi.org/10.1016/j.jmmm.2014.02.050. URL ⟨http://www.sciencedirect.com/science/article/pii/S0304885314001620⟩.

[12] G. Kreiner, A. Kalache, S. Hausdorf, V. Alijani, J.-F. Qian, G. Shan, U. Burkhardt, S. Ouardi, C. Felser, New Mn_2-based Heusler compounds, Z. Anorg. Allg. Chem. 640(5) (2014) 738–752. http://dx.doi.org/10.1002/zaac.201300665. URL ⟨http://dx.doi.org/10.1002/zaac.201300665⟩.

[13] H. Han, Z. Bai, K.L. Yao, Half-metallicity of bulk and (1 1 1) surface for full-heusler alloy Co_2VAl: a density functional study, J. Alloys Compd. 576(0) (2013) 93–97. http://dx.doi.org/http://dx.doi.org/10.1016/j.jallcom.2013.04.145. URL ⟨http://www.sciencedirect.com/science/article/pii/S0925838813010669⟩.

[14] I. Galanakis, P. Mavropoulos, Zinc-blende compounds of transition elements with N, P, As, Sb, S, Se, and Te as half-metallic systems, Phys. Rev. B: Condens. Matter Mater. Phys. 67(10) (2003) 104417. URL ⟨http://link.aps.org/doi/10.1103/PhysRevB.67.104417⟩.

[15] M. Bibes, A. Barthelemy, Oxide spintronics, IEEE Trans. Electron Devices 54 (5) (2007) 1003–1023, http://dx.doi.org/10.1109/TED.2007.894366.

[16] F. Natali, B.J. Ruck, N.O.V. Plank, H.J. Trodahl, S. Granville, C. Meyer, W.R.L. Lambrecht, Rare-earth mononitrides, Prog. Mater. Sci. 58(8) (2013) 1316–1360. http://dx.doi.org/http://dx.doi.org/10.1016/j.pmatsci.2013.06.002. URL ⟨http://www.sciencedirect.com/science/article/pii/S007964251300056X⟩.

[17] E.V. Gomonay, V.M. Loktev, Spintronics of antiferromagnetic systems, Low Temp. Phys. 40(1) (2014) 17–35. http://dx.doi.org/10.1063/1.4862467. URL ⟨http://scitation.aip.org/content/aip/journal/ltp/40/1/10.1063/1.4862467⟩.

[18] A.B. Shick, S. Khmelevskyi, O.N. Mryasov, J. Wunderlich, T. Jungwirth, Spin–orbit coupling induced anisotropy effects in bimetallic antiferromagnets: a route towards antiferromagnetic spintronics, Phys. Rev. B 81 (21) (2010) 212409.

[19] V.M.T.S. Barthem, C.V. Colin, H. Mayaffre, M.H. Julien, D. Givord, Revealing the properties of Mn_2Au for antiferromagnetic spintronics, Nat. Commun. 4 (2013) 2892.

[20] T. Yamanaka, Y. Komatsu, H. Nomori, Electron density distribution of $FeTiO_3$ ilmenite under high pressure analyzed by MEM using single crystal diffraction intensities, Phys. Chem. Miner. 34 (5) (2007) 307–318, http://dx.doi.org/10.1007/s00269-007-0149-7.

[21] E.J. Tronche, J. Van Kan Parker, J. Vries, Y. Wang, T. Sanehira, J. Li, B. Chen, L. Gao, S. Klemme, McCammon, W. van Westrenen, The thermal equation of state of $FeTiO_3$ilmenite based on in situ X-ray diffraction at high pressures and temperatures, Am. Mineral. 95 (2010) 1708–1716. ⟨http://ammin.geoscienceworld.org/content/95/11-12/1708.abstract⟩.

[22] G.B. Andreozzi, F. Cellucci, D. Gozzi, High-temperature electrical conductivity of $FeTiO_3$ and ilmenite, J. Mater. Chem. 6 (6) (1996) 987–991, http://dx.doi.org/10.1039/JM9960600987.

[23] W. Xiao, X.-G. Lu, X.-L. Zou, X.-M. Wei, W.-Z. Ding, Phase transitions, micromorphology and its oxidation mechanism in oxidation of ilmenite ($FeTiO_3$) powder, Trans. Nonferrous Metals Soc. China 23(8) (2013) 2439–2445. http://dx.doi.org/http://dx.doi.org/10.1016/S1003-6326(13)62752-1. URL ⟨http://www.sciencedirect.com/science/article/pii/S1003632613627521⟩.

[24] Y.J. Kim, B. Gao, S.Y. Han, M.H. Jung, A.K. Chakraborty, T. Ko, C. Lee, W.I. Lee, Heterojunction of $FeTiO_3$ nanodisc and TiO_2 nanoparticle for a novel visible light photocatalyst, J. Phys. Chem. C 113 (44) (2009) 19179–19184, http://dx.doi.org/10.1021/jp908874k.

[25] S. Ohara, K. Sato, Z. Tan, H. Shimoda, M. Ueda, T. Fukui, Novel mechanochemical synthesis of fine $FeTiO_3$ nanoparticles by a high-speed ball-milling process, J. Alloys Compd. 504(1) (2010) L17–L19. http://dx.doi.org/http://dx.doi.org/10.1016/j.jallcom.2010.05.090. URL ⟨http://www.sciencedirect.com/science/article/pii/S0925838810012727⟩.

[26] T. Tao, A.M. Glushenkov, H. Liu, Z. Liu, X.J. Dai, H. Chen, S.P. Ringer, Y. Chen, Ilmenite $FeTiO_3$ nanoflowers and their pseudocapacitance, J. Phys. Chem. C 115 (35) (2011) 17297–17302, http://dx.doi.org/10.1021/jp203345s.

[27] A.T. Raghavender, N. Hoa Hong, K. Joon Lee, M.-H. Jung, Z. Skoko, M. Vasilevskiy, M.F. Cerqueira, A.P. Samantilleke, Nano-ilmenite $FeTiO_3$: synthesis and characterization, J. Magn. Magn. Mater. 331 (2013) 129–132. http://dx.doi.org/http://dx.doi.org/10.1016/j.jmmm.2012.11.028. URL ⟨http://www.sciencedirect.com/science/article/pii/S0304885312009316⟩.

[28] D. Nakatsuka, T. Yoshino, J. Kano, H. Hashimoto, M. Nakanishi, J. Takada, T. Fujii, High-pressure synthesis, crystal structure and magnetic property of ilmenite-type $FeGeO_3$, J. Solid State Chem. 198 (2013) 520–524. http://dx.doi.org/http://dx.doi.org/10.1016/j.jssc.2012.11.020. URL ⟨http://www.sciencedirect.com/science/article/pii/S0022459612007049⟩.

[29] A. Stashans, L. Eras, G. Chamba, Modelling of Al impurity in perovskite and ilmenite structures of $MgSiO_3$, Phys. Chem. Miner. 37(4) (2010) 191–199. http://dx.doi.org/10.1007/s00269-009-0323-1. URL ⟨http://dx.doi.org/10.1007/s00269-009-0323-1⟩.

[30] T. Okada, T. Narita, T. Nagai, T. Yamanaka, Comparative Raman spectroscopic study on ilmenite-type $MgSiO_3$ (akimotoite), $MgGeO_3$, and $MgTiO_3$ (geikielite) at high temperatures and high pressures, Am. Mineral. 93 (2008) 39–47.

[31] N.-N. Ge, C.-M. Liu, Y. Cheng, X.-R. Chen, G.-F. Ji, First-principles calculations for elastic and electronic properties of $ZnSnO_3$ under pressure, Phys. B (Amsterdam, Neth.) 406(4) (2011) 742–748. http://dx.doi.org/http://dx.doi.org/10.1016/j.physb.2010.11.046. URL ⟨http://www.sciencedirect.com/science/article/pii/S0921452610011014⟩.

[32] K.E.H.M. Hanssen, P.E. Mijnarends, Positron-annihilation study of the half-metallic ferromagnet NiMnSb: theory, Phys. Rev. B: Condens. Matter Mater. Phys. 34(8) (1986) 5009–5016. ⟨http://link.aps.org/doi/10.1103/PhysRevB.34.5009⟩.

[33] K.E.H.M. Hanssen, P.E. Mijnarends, L.P.L.M. Rabou, K.H.J. Buschow, Positron-annihilation study of the half-metallic ferromagnet NiMnSb: experiment, Phys. Rev. B: Condens. Matter Mater. Phys. 42(3) (1990) 1533–1540. ⟨http://link.aps.org/doi/10.1103/PhysRevB.42.1533⟩.

[34] R. Huber, P. Klemm, S. Neusser, B. Botters, A. Wittmann, M. Weiler, S.T.B. Goennenwein, C. Heyn, M. Schneider, P. Bni, D. Grundler, Advanced techniques for all-electrical spectroscopy on spin caloric phenomena, Solid State Commun. 150(11–12) (2010) 492–495. http://dx.doi.org/http://dx.doi.org/10.1016/j.ssc.2009.11.020. URL ⟨http://www.sciencedirect.com/science/article/pii/S0038109809007091⟩.

[35] F.D. Czeschka, L. Dreher, M.S. Brandt, M. Weiler, M. Althammer, I.M. Imort, G. Reiss, A. Thomas, W. Schoch, W. Limmer, H. Huebl, R. Gross, S.T.B. Goennenwein, Scaling behavior of the spin pumping effect in ferromagnet-platinum bilayers, Phys. Rev. Lett. 107(4) (2011) 046601. ⟨http://link.aps.org/doi/10.1103/PhysRevLett.107.046601⟩.

[36] A.D. Becke, Density-functional thermochemistry. III: the role of exact exchange, J. Chem. Phys. 98 (7) (1993) 5648–5652.

[37] A.D. Becke, Density-functional exchange-energy approximation with correct asymptotic behavior, Phys. Rev. A: At. Mol. Opt. Phys. 38(6) (1988) 3098–3100. URL ⟨http://link.aps.org/doi/10.1103/PhysRevA.38.3098⟩.

[38] C. Lee, W. Yang, R.G. Parr, Development of the Colle–Salvetti correlation-energy formula into a functional of the electron density, Phys. Rev. B: Condens. Matter Mater. Phys. 37(2) (1988) 785–789. URL ⟨http://link.aps.org/doi/10.1103/PhysRevB.37.785⟩.

[39] R. Dovesi, R. Orlando, B. Civalleri, C. Roetti, V.R. Saunders, C.M. Zicovich-Wilson, CRYSTAL: a computational tool for the ab initio study of the electronic properties of crystals, Z. Kristallogr. New Cryst. Struct 220 (2005) 571–573.

[40] M.F. Peintinger, D.V. Oliveira, T. Bredow, Consistent gaussian basis sets of triple-zeta valence with polarization quality for solid-state calculations, J. Comput. Chem. 34 (6) (2013) 451–459, http://dx.doi.org/10.1002/jcc.23153.

[41] P. Durand, J.-C. Barthelat, A theoretical method to determine atomic pseudopotentials for electronic structure calculations of molecules and solids, Theor. Chim. Acta 38 (4) (1975) 283–302, http://dx.doi.org/10.1007/BF00963468.

[42] M. Causà, R. Dovesi, C. Roetti, Pseudopotential Hartree–Fock study of seventeen III-V and IV-IV semiconductors, Phys. Rev. B: Condens. Matter Mater. Phys. 43(14) (1991) 11937–11943. ⟨http://link.aps.org/doi/10.1103/PhysRevB.43.11937 ⟩.

[43] B.A. Wechsler, C.T. Prewitt, Crystal structure of ilmenite ($FeTiO_3$) at high temperature and at high pressure, Am. Mineral. 69 (1984) 176–185.

[44] H.J. Monkhorst, J.D. Pack, Special points for Brillouin-zone integrations, Phys. Rev. B: Condens. Matter Mater. Phys. 13(12) (1976) 5188–5192. ⟨http://link.aps.org/doi/10.1103/PhysRevB.13.5188⟩.

[45] N.C. Wilson, J. Muscat, D. Mkhonto, P.E. Ngoepe, N.M. Harrison, Structure and properties of ilmenite from first principles, Phys. Rev. B: Condens. Matter Mater. Phys. 71(7) (2005) 075202. ⟨http://link.aps.org/doi/10.1103/PhysRevB.71.075202⟩.

[46] M. Getzlaff, Fundamentals of Magnetism, Springer-Verlag, Berlin, 2008.

[47] B.G. Park, J. Wunderlich, X. Mart, V. Hol, Y. Kurosaki, M. Yamada, H. Yamamoto, A. Nishide, J. Hayakawa, H. Takahashi, A.B. Shick, T. Jungwirth, A spin-valve-like magnetoresistance of an antiferromagnet-based tunnel junction, Nat. Mater. 10 (5) (2011) 347–351, http://dx.doi.org/10.1038/nmat2983.

[48] S. Nazir, N. Singh, M. Upadhyay-Kahaly, U. Schwingenschlogl, Role of the electronegativity for the interface properties of non-polar heterostructures, Europhys. Lett. 98(2) (2012) 27007. http://dx.doi.org/10.1209/0295-5075/98/27007. URL ⟨http://dx.doi.org/10.1209/0295-5075/98/27007⟩.

[49] M. Toyoda, K. Yamauchi, T. Oguchi, Ab initio study of magnetic coupling in $CaCu_3B_4O_{12}$ (B = Ti, Ge, Zr, and Sn), Phys. Rev. B. 87(22) (2013) 224430. http://dx.doi.org/10.1103/PhysRevB.87.224430. URL ⟨http://link.aps.org/doi/10.1103/PhysRevB.87.224430⟩.

[50] A.Y. Dantsiger, O.N. Razumovskaya, L.A. Reznichenko, S.I. Dudkina, L. A. Shilkina, A.N. Klevtsov, Effects of B-cation electronegativity and B–O bond covalence on the properties of multicomponent solid solutions based on Lead Zirconate Titanate, Inorg. Mater. 37 (12) (2001) 1294–1297, http://dx.doi.org/10.1023/A:1012986311389.

[51] D.D. Awschalom, M.E. Flatte, Challenges for semiconductor spintronics, Nat. Phys. 3 (3) (2007) 153–159.

[52] T. Dietl, H. Ohno, Dilute ferromagnetic semiconductors: physics and spintronic structures, Rev. Mod. Phys. 86 (1) (2014) 187–251.

[53] M. Kuno, Density of States, 1st edition, Gerland Science, Oxford, 2011, book 9, pp. 203–237.